WEP Warwick Evans Publishing

International Journal of Computer Science and Information Technology

ISSN: 3005-9682 (Print), ISSN: 3005-7140 (Online) | Volume 2, Number 3, Year 2024
DOI: https://doi.org/10.62051/ijcsit.v2n3.10
Journal homepage: https://wepub.org/index.php/IJCSIT/index

Research on AGV Global Positioning Algorithm Based on Reflector and Lidar

Yunlong Zhao[1,*], Peng Jin[2], Qingyuan Huang[3]

[1]Sichuan University of Science & Engineering, Yibin, China

[2]Sichuan Guoguang Agrochemical Co., Ltd, Chengdu, China

[3]Sichuan University of Science & Engineering, Yibin, China

*Corresponding Author: Yunlong Zhao

ABSTRACT

In order to improve the accuracy, stability, and robustness of AGV positioning with the use of the Cartographer algorithm, this paper proposes a global positioning algorithm strategy that integrates the reflector coordinate points as reference points for the trilateral positioning algorithm with the cartographer. Firstly, the shortcomings of existing cartographers in pure positioning were introduced. Then, two commonly used positioning algorithms were elaborated, and they were fused using reflective plates and cartographer algorithms. Static and dynamic experiments were conducted in real environments. The two experiments verified that the trilateral positioning algorithm has smaller errors, stronger stability, and better accuracy than the triangular positioning algorithm.

KEYWORDS

AGV; Cartographer algorithm; location; Reflective panel

1. INTRODUCTION

With the continuous negative population growth and the development of aging population in China, mobile robots, as the most intelligent product that can replace the demand for human resources and industrial upgrading in various industries, are in increasing demand in various industries[1]. According to data from the CMR Industry Alliance, the sales of mobile robots (AGV/AMR) in China have been increasing year by year from 2015 to 2022. In 2022, the market size of mobile robots (AGV/AMR) reached 18.5 billion, a year-on-year increase of 46.82%[2]. In 2023, the Ministry of Industry and Information Technology, in collaboration with 17 departments, released the Implementation Plan for the "Robot+" Application Action, proposing to provide long-term support for the development of China's robotics industry and promote the upgrading and transformation of various industries[3]. With the gradual maturity of robotics related technologies in the past decade, it has also laid a solid foundation for promoting the industrialization of robotic humans[4].

In the early days, AGV only carried out cargo transportation along designated routes[5]. Later, the development of SLAM related technologies played a key role in promoting AGV autonomous navigation[6]. AGV use sensors such as LiDAR or cameras to perceive the surrounding environment for mapping, while also determining their own position or positioning[7]. The quality of mapping directly affects the subsequent path planning of AGVs. Therefore, research on SLAM technology is gradually becoming a path for the future development of AGV.

In response to the difficulties in determining positioning loss or coordinate jumps that occur in indoor environments during pure positioning using the Cartographer algorithm, this article solves the

problem by adding reflective panels in the environment as landmarks in the Cartographer algorithm[8]. Firstly, in the case where the reflectivity of the reflective panel does not decrease in recognition according to the manufacturer's curve, a reduction ratio coefficient is set, as well as some reflection intensity thresholds and distance thresholds. Experimental verification was conducted on commonly used positioning algorithms, including trilateral positioning algorithm and triangular positioning algorithm. The experiments in both stationary and moving states of AGV confirmed that the trilateral positioning accuracy based on reflective panels is higher and more stable.

2. SYSTEM COMPOSITION AND REFLECTOR LAYOUT REQUIREMENTS

2.1. Composition of laser positioning system

AGV needs the support of its own hardware conditions to complete the operation, this paper will select the chassis and LIDAR sensors related to AGV suitable for indoor operation.

The chassis is the carrier of AGV LIDAR and other sensors and the main body of the AGV, but also the basic form of the mobile robot. Mobile robots can usually be wheeled and footed for movement, robots that move by motor-driven wheels are wheeled robots, and robots that move by bionic multi-legged joints are multi-legged robots[9]. Because of the complexity of controlling multi-legged robots, wheeled robots are more commonly used in commercial applications.

Wheeled robot chassis can be categorized into two-wheeled differential model, four-wheeled differential model, Ackermann model, omnidirectional model, etc. according to the steering method . The two-wheel differential model, four-wheel differential model, and Ackermann model are also known as motion-constrained models, and the omnidirectional model is also known as motion-unconstrained model[10].

The advantages and disadvantages of its specific chassis kinematic model are shown in Table 2-2. Overall, based on the comparison, most of the environment in which the AGV operates is a factory environment, and the motion mode is not constrained in many aspects. Therefore, an omnidirectional model is chosen to construct the AGV chassis[11]. In addition to the selection of the chassis model, there are also considerations for the installation method of the McNamp wheels in its model. The commonly used installation methods are shown in Figure 1, mainly the X-type installation method and the O-type installation method. Due to the fact that the X-type installation method is not as long as the O-type installation method in generating shaft rotation torque, it is limited in some AGV movements. Therefore, the O-type installation method is a common installation method. Therefore, in this article, the O-type installation method is also chosen when installing the McNamp.

Table 1. Comparison of advantages and disadvantages of common chassis models

Chassis model	Motion constraint situation	Minimum turning radius	Mileage meter accuracy	Trajectory tracking
Two wheel differential model	Constrained	0	high	easily
Four wheel differential model	Constrained	0	low	complex
Ackermann model	Constrained	Non 0	secondary	complex
Omnidirectional model	Unconstrained	0	secondary	easily

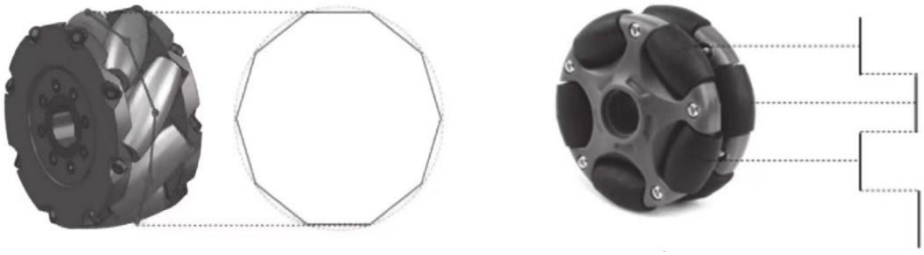

(a) Roller 45°type (b) Roller 90°type

Figure 1. McNamm wheel type diagram

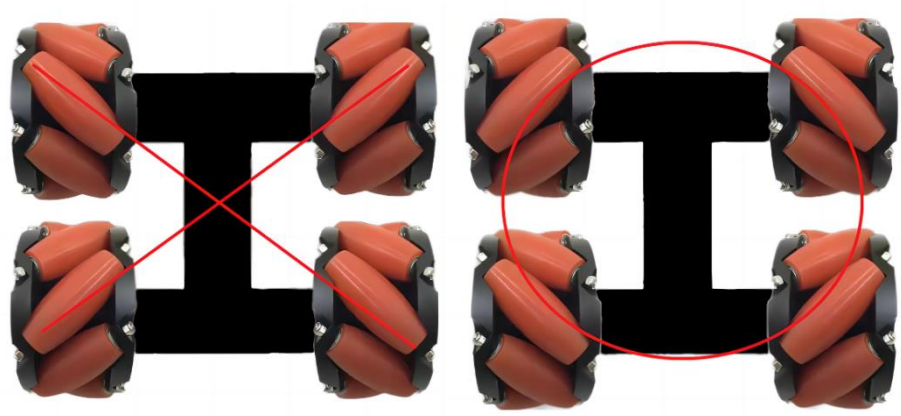

(a) X-shaped installation method (b) O-shaped installation method

Figure 2. McNamm wheel installation diagram

2.2. Reflector arrangement requirements

When the LIDAR carried by the AGV scans for information in the factory environment, the light emitted by it is reflected by most of the objects in the factory environment, but the intensity of the reflected light varies on different objects. The reflection intensity of the reflector is higher than that of other objects in the positioning environment, so it is necessary to distinguish between the reflector and other objects according to the intensity of the reflected laser signal. Since AGVs need the position and angle information of reflectors from LIDAR for positioning and mapping, the selection of reflective strength of reflectors in the positioning environment, the placement of reflectors, as well as the number and size of reflectors will all affect their positioning effect.

According to the positioning environment in which the AGV is located and the height between the LIDAR and the reflector, it is necessary to make some requirements for the arrangement of the reflector, which are as follows:

(1) The distance between two reflectors should be more than 500mm;

(2) The arrangement between the reflectors can not be symmetrical, and is required to be distributed on both sides of the driving path, and not equally spaced distribution arrangement;

(3) In the driving path throughout the need to be able to detect at least three reflectors, and throughout the laser to the two reflectors between the angle is greater than 3 °;

(4) in the reflective strip installation, should try to ensure that there is no high reflectivity objects nearby (including other reflective strips, or glass mirrors), reflective strips and high reflectivity objects should be guaranteed between the distance of more than 100cm, if the reflective strips of the width or diameter of the larger, then the corresponding distance should be greater, and at the same

time placing reflective columns when usually placed away from the back of the background object distance is less than 10cm.

(5) in the field layout reflector, should try to ensure that the center height of the reflective strip and laser level height consistent, and leave a certain margin above and below, to ensure that the movement of the laser can still be irradiated on the reflector. Usually need to ensure that the height of the reflective column in more than 50cm, to ensure that in the farther, can still operate normally. In the ground AGV use, due to AGV usually laser installation from the ground height is low, at the same time need to pay attention to the laser installation angle, and due to the ground is not flat enough will lead to changes in the laser level, so usually need to AGV driving ground to meet the FF50 (ACI 117 standard), that is, 3m ruler error in +3mm, this is a relatively easy to achieve the degree of flatness. This is an easy leveling level to achieve.

3. GLOBAL POSITIONING ALGORITHM

3.1. Triangulation algorithm

Triangle positioning algorithm is through the two reflectors and AGV for the three vertices constructed into a triangle, through the trigonometric function and the coordinates of the reflector information to calculate the position information of the AGV[12], its specific positioning principle shown in Figure 3,Assuming that the AGV is the vertex O in the figure, and the other two reflectors are P_1 and P_2, the LIDAR accepts the information of the reflectors P_1 and P_2 and can calculate OP_1 and OP_2, the number of reflectors in the environment should be greater than or equal to two, due to the position of the reflectors in the localization environment is laid out in advance, so the distance P_1P_2 between the two reflectors can be calculated. From the trigonometric function can be derived from the angle information, and set $\angle OP_1P_2$ and $\angle OP_2P_1$ the angle were α and β, in order to be more intuitive representation, from the position of the AGV to the line between the two reflectors to make a plumb line P_1P_2 and set to d, so that P_1P_2 the mathematical expression can be obtained for the formula 1.

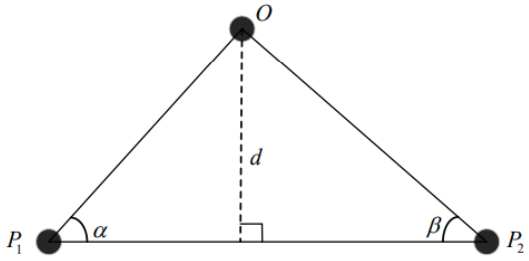

Figure 3. Diagram of Triangle Positioning Algorithm

$$P_1P_2 = \frac{d}{\tan\alpha} + \frac{d}{\tan\beta} = d\left(\frac{1}{\tan\alpha} + \frac{1}{\tan\beta}\right) \tag{1}$$

It is obtained by simplifying 3 from trigonometric functions and their formulas:

$$P_1P_2 = d\frac{\sin(\alpha+\beta)}{\sin\alpha\sin\beta} \tag{2}$$

$$d = P_1P_2\frac{\sin\alpha\sin\beta}{\sin(\alpha+\beta)} \tag{3}$$

Given the coordinates of the reflector in the global coordinate system, the position coordinates of the AGV can be calculated based on the robot's coordinate transformation relationship[13]. When there are multiple reflectors in the actual environment, in order to save computational costs and improve computational accuracy, the actual solution method is to use the least squares method to obtain the coordinate information of AGV.

3.2. Trilateral localization algorithm

The positioning algorithm used in this article is the trilateral positioning algorithm. The principle of the trilateral positioning algorithm [14] is to establish a circle with a reflector as the center and the relative distance between the AGV and the reflector as the radius. The number of reflectors must be greater than or equal to three, but in practical use, they are all greater than three. The AGV position is determined by the intersection point of the circle constructed by the reflector. The ideal situation is shown in Figure 4, where points A, B, and C represent the position of the reflector, and the radii of the circles constructed by points A, B, and C are r_A 、 r_B and r_C , respectively, and the intersection point P represents the position of the AGV[15]. The formula for calculating the radius of the reflector circle and the AGV coordinate relationship is shown in equations 4. In case a, the deflection angle of one of the reflectors (represented by reflector A here) can be calculated using the position coordinates of the AGV. The deflection angle of the other two reflectors can also be calculated using this calculation method. After knowing the deflection angles of three reflective panels, the average deflection angle of AGV can be obtained as shown in Equation 5.

$$\begin{cases} (x_P - x_A)^2 + (y_P - y_A)^2 = r_A^2 \\ (x_P - x_B)^2 + (y_P - y_B)^2 = r_B^2 \\ (x_P - x_C)^2 + (y_P - y_C)^2 = r_C^2 \end{cases} \tag{4}$$

$$\theta_A = \arctan\frac{x_A - x_P}{y_A - y_P} - \varphi_A \tag{5}$$

$$\theta_P = \frac{1}{3}\left(\theta_A + \theta_B + \theta_C\right) \tag{6}$$

$$\theta_P = \frac{1}{3}\left(\theta_A + \theta_B + \theta_C\right) \tag{7}$$

he above is an ideal scenario where the position information of AGV is determined through the trilateral positioning algorithm. However, in practical situations, due to various errors, it can lead to the situation in Figure 4 where the circle constructed by the reflector cannot be compared to a single point, where the circles constructed by the reflector intersect in an area, the circles constructed by the reflector do not intersect, and AGV scans more than three reflectors[16]. The above equation cannot be solved. At this point, an approximate solution needs to be obtained using the least squares method to calculate the position of the AGV[14]. The distance calculation method is as follows:

$$\begin{cases} (x_P - x_1)^2 + (y_P - y_1)^2 = r_1^2 \\ \vdots \\ (x_P - x_n)^2 + (y_P - y_n)^2 = r_n^2 \end{cases} \tag{8}$$

Through simplification:

$$AX_P = b \tag{9}$$

In formula 9:

$$A = \begin{bmatrix} 2(x_1 - x_n) & 2(y_1 - y_n \\ \vdots & \vdots \\ 2(x_{n-1} - x_n) & 2(y_{n-1} - y_n) \end{bmatrix} \tag{10}$$

$$b = \begin{bmatrix} x_1^2 - x_n^2 + y_1^2 - y_n^2 + r_n^2 - r_1^2 \\ \vdots \\ x_{n-1}^2 - x_n^2 + y_{n-1}^2 - y_n^2 + r_n^2 - r_{n-1}^2 \end{bmatrix} \tag{11}$$

Solving formula 11 yields:

$$X_P = (A^{\mathrm{T}} A)^{-1} A^{\mathrm{T}} b \tag{12}$$

The final formula for calculating the deflection angle of AGV is:

$$\theta_P = \frac{1}{n} \sum_{n}^{i=1} \arctan \frac{x_i - x_P}{y_i - y_P} - \varphi_i \tag{13}$$

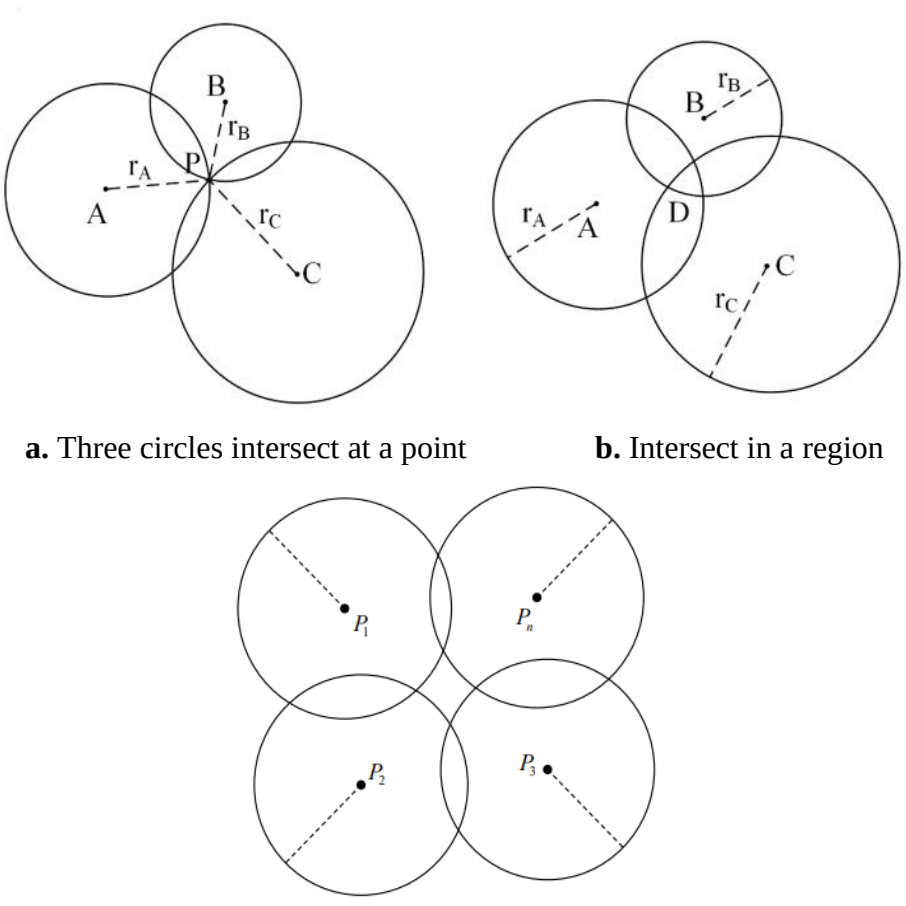

a. Three circles intersect at a point **b.** Intersect in a region

c. Circles cannot intersect

Figure 4. Principle of Trilateral Positioning Algorithm

4. REAL ENVIRONMENT EXPERIMENT

Building reflective panels in a real environment for verification based on global positioning experiments using reflective panels. The positioning experiments compared the algorithms using

trilateral positioning algorithms and triangular positioning algorithms. The two experiments were static positioning experiments and dynamic positioning experiments, and the performance of the two positioning algorithms was analyzed.

4.1. Experimental environment and configuration

The real experimental environment is the factory production workshop environment, as shown in Figure 5. The configuration requirement is to build an AGV car independently, as shown in Figure 6. In a larger map environment, the LiDAR used is shown in Figure 7. The computer configuration environment is Intel's seventh generation I5, and the graphics card is MX250.

Figure 5. Real factory environment

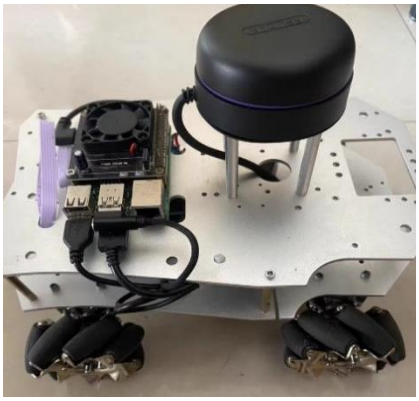

Figure 6. Self built AGV

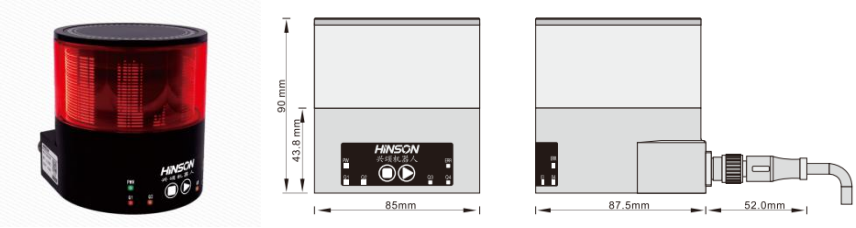

Figure 7. Lidar used in the general environment

4.2. Static positioning experiment

In this experiment, the AGV was placed stationary in an environment covered with reflective panels, and its ROS localization node topic is shown in Figure 4-8. By manufacturing a landmark on the reflective panel for localization, the AGV's pose was measured to be: X=12.00m, Y=10.00m, θ=

0.150rad, by recording the trilateral positioning algorithm and triangular positioning algorithm, the bag data in the ROS is shown in Figure 4-9. After collecting the data, the plot is shown in Figure 4-10. The black and gray dots represent the trilateral positioning data based on the reflector, and the red dots represent the triangular positioning data based on the reflector. Comparing the three dimensions of a, b, and c in the figure, it can be seen that the black dots are closer to the real data. Although the red dots are more concentrated, they appear farther away from the real data. In d, it can be seen that the gray dots are more concentrated on the real data, and the red dots are more scattered on the edges of the real data. The performance of the graph proves that trilateral positioning is more accurate than triangular positioning. More precise and stable.

Calculate the average and variance of the obtained experimental data, as shown in Table 2. Through data analysis in the table, it is found that in static positioning, the three sided positioning based on reflective panels is more effective than the triangular positioning based on reflective panels in X, Y, and θ The upper error should be small, and the positioning accuracy should be high. Through variance data comparison, the three-sided positioning based on reflective panels is more stable than the triangular positioning based on luminous panels.

The black dots in the figure represent the trilateral positioning algorithm based on reflective panels, while the red dots represent the triangular positioning algorithm based on reflective panels.

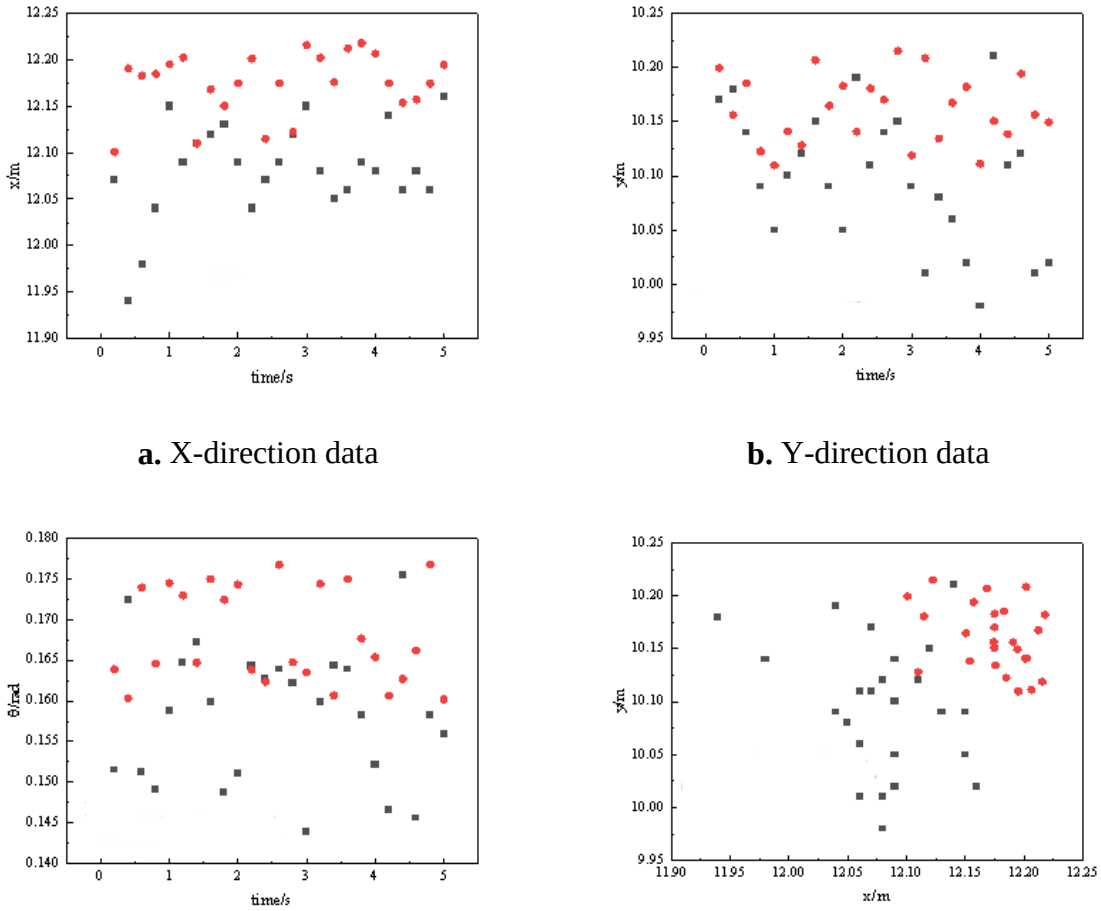

a. X-direction data

b. Y-direction data

c. Yaw angle data

d. X-Y data

Figure 8. Static positioning data analysis of two positioning algorithms

Table 2. Calculation of mean and variance of two localization algorithms

Positioning algorithm	Trilateral positioning algorithm based on reflective panels			Triangle positioning algorithm based on reflective panels		
	X	Y	θ	X	Y	θ
average value	12.082	10.0976	0.15808	12.1714	10.1606	0.1678
variance	0.22298	0.24579	0.09033	0.18075	0.17533	0.07607

4.3. Dynamic experiment

In the dynamic positioning experiment, in order to compare the performance of the two algorithms in multiple aspects, a route was set as shown below. The trajectory map displayed in the ROS is shown in 4-11, where the reflector position and the preset route are shown in c, and the trilateral positioning and triangular positioning are shown in a and b, respectively. After collecting the bag data recorded in ROS, a comparison chart is drawn as shown in 4-12. The black and gray lines in the chart represent the preset path data, the red lines represent the three edge positioning data based on the reflector, and the blue lines represent the triangle positioning data based on the reflector. The preset path includes three actions: X straight, Y straight, and turning, which facilitates the analysis and comparison of the two algorithms for the three angles.

In the X straight section, it can be clearly seen that the trilateral positioning algorithm is closer to the planned preset path compared to the triangular positioning algorithm. In the Y straight section, the triangular positioning algorithm shows obvious shaking, which may be due to the fact that the two selected reflectors are more affected by the environment during AGV driving, while the trilateral positioning algorithm is relatively stable. This is because the trilateral positioning selects three reflectors, which leads to a higher fault tolerance rate. At the turning point, the data collected by the triangular positioning algorithm overlaps and shakes significantly due to the influence of AGV's own speed and other factors. This is because the positions of the two selected reflectors during AGV rotation are not changed to new reflectors as points for determination during turning. However, the trilateral localization algorithm performed well without significant overlap or jitter, Therefore, in the dynamic positioning experiment, it can be concluded that the accuracy and stability of the trilateral positioning algorithm are higher than those of triangular positioning.

In Figure 10, red represents the trilateral positioning algorithm based on reflective panels, blue represents the triangular positioning algorithm based on reflective panels, and gray represents the AGV preset path.

Based on the static positioning experiment in the previous section, it can be concluded that regardless of whether AGV is positioned when prohibited or when completing tasks, the accuracy and stability of the trilateral positioning algorithm based on reflectors are superior to those based on reflectors.

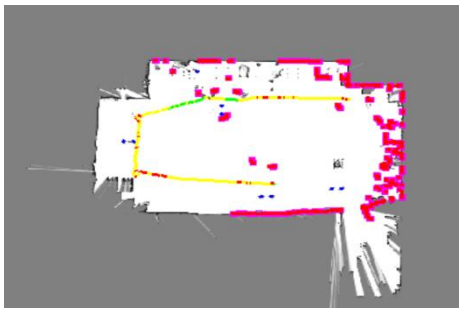

a. Trilateral positioning

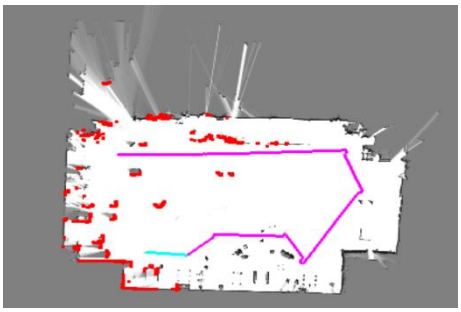

b. Triangle positioning

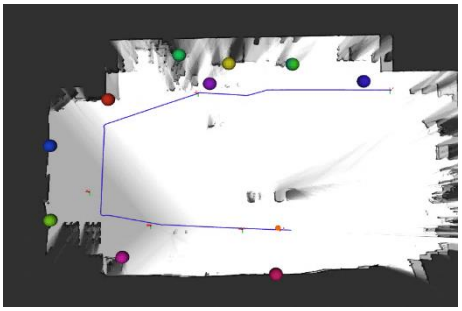

c.default route

Figure 9. Positioning trajectory diagram in ros environment

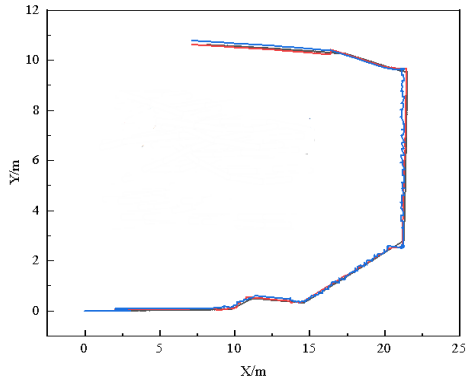

Figure 10. Two algorithms for locating data analysis

5. SUMMARY

This article is a study on the global positioning method based on reflective panels. In response to the difficulties in determining positioning loss or coordinate jumps that occur in indoor environments during pure positioning using the Cartographer algorithm, this article solves the problem by adding reflective panels in the environment as landmarks in the Cartographer algorithm. Firstly, in the case where the reflectivity of the reflective panel does not decrease in recognition according to the manufacturer's curve, a reduction ratio coefficient is set, as well as some reflection intensity thresholds and distance thresholds. Experimental verification was conducted on commonly used positioning algorithms, including trilateral positioning algorithm and triangular positioning algorithm. Firstly, requirements and precautions were made for the layout environment of reflective panels. Secondly, the extraction and matching of reflective panels were explained. Then, the principles and formula derivation of the two positioning algorithms, trilateral positioning algorithm and triangular positioning algorithm, were explained. Finally, experiments were conducted on the stationary and moving states of the AGV in a reflective panel environment. Three scenarios were designed for the moving state: X straight, Y straight, and turning. Two sets of experiments have demonstrated that the

trilateral positioning algorithm based on reflective panels has higher accuracy and stronger stability. The experiments in both stationary and moving states of AGV have verified that the three-sided positioning accuracy based on reflective panels is higher and more stable.

ACKNOWLEDGEMENTS

Supported by The Innovation Fund of Postgraduate, Sichuan University of Science & Engineering.

REFERENCES

[1] CHEN LIANG, KUUSNIEMI H, CHEN YUWEI, et al. Information filter with speed detection for indoor bluetooth positioning[C]//The Institute of Electrical and Electronic Engineers (IEEE). Proceedings of 2011 International Conference on Localization and GNSS (ICL-GNSS). Tampere, Finland: IEEE, 2011:47-52.

[2] NAOYA OHNISHI, ATSUSHI IMIYA. Appearance-based navigation and homing for autonomous mobile robot[J]. Image and Vision Computing, 2013, 31(6-7): 511-532.

[3] QI L, LIU Y, YU Y, et al. Current Status and Future Trends of Meter-Level Indoor Positioning Technology: A Review [J]. Remote Sensing, 2024, 16(2):58-64.

[4] DIJKSTRA E W. A note on two problems in connection with graphs[J] Springer Science and Business Media LLC, 1959, 1(1): 269-271.

[5] SINCLAIR J B. Optimal assignments in broadcast networks[J]. IEEE Transactions on Computers, 1988, 37(5):521-531.

[6] COLLE E, GALERNE S. Mobile robot localization by multinucleation using set inversion[J]. Robotics and Autonomous Systems, 2012, 61(1): 39-48.

[7] HEUSS L, GONNERMANN C, REINHART G. An extendable framework for intelligent and easily configurable skills-based industrial robot applications[J]. The International Journal of Advanced Manufacturing Technology, 2022, 120(9-10): 6269-6285.

[8] ALEXANDRA KIRSCH. Shakey Ever After Questioning Tacit Assumptions in Robotics and Artificial Intelligence[J]. 2019, 33(04): 423-428.

[9] YUN-SU HA, SHINICHI YUTA. Trajectory tracking control for navigation of the inverse pendulum type self-contained mobile robot [J]. 1996, 17(01): 65-80.

[10] DISSANAYAKE M W M G, NEWMAN P, CLARK S, et al. A solution to the simultaneous localization and map building (SLAM) problem[J]. IEEE Transactions on robotics and automation, 2001, 17(3): 229-241.

[11] HUANG G P, MOURIKIS A I, ROUMELIOTISS I. Analys is and improvement of the consistency of extended Kalman filter based SLAM[C]//IEEE International Conference on Robotics and Automation. IEEE, 2008: 473-479.

[12] K. MURPHY. Bayesian map learning in dynamic environments.[J] Neural Inf. Process. Syst, 1999: 1015–1021.

[13] GRISETTI G, STACHNISS C, BURGARD W. Improved techniques for grid mapping with Rao-Blackwell zed particle filters[J]. IEEE Transactions on Robotics, 2007, 23(1): 34-46.

[14] BEKRAR A, KACEM I, CHU C, et al. A branch and bound algorithm for solving the 2D strip packing problem[C]// 2006 International Conference on Service Systems and Service Management, Troyes, France, 2006: 940-946

[15] SFEIR J, SAAD M, SALIAH-HASSANE H. An improved artificial potential field approach to real-time mobile robot path planning in an unknown environment[C]//IEEE International Symposium on Robotic and Sensors Environments (ROSE), IEEE, 2011: 208-213.

[16] ADAMU P IOKAGBUE H IOGUNTUNDE P E. Fast and optimal path planning algorithm (FAOPPA) for a mobile robot[J]. Wireless Personal Communications, 2019, 106(2): 577-592.